Korean Journal of Remote Sensing, Vol.24, No.3, 2008, pp.257~267

Quadratic Programming Approach to Pansharpening of Multispectral Images Using a Regression Model

Sang-Hoon Lee †

Kyungwon University

Abstract : This study presents an approach to synthesize multispectral images at a higher resolution by exploiting a high-resolution image acquired in panchromatic modality. The synthesized images should be similar to the multispectral images that would have been observed by the corresponding sensor at the same high resolution. The proposed scheme is designed to reconstruct the multispectral images at the higher resolution with as less color distortion as possible. It uses a regression model of the second order to fit panchromatic data to multispectral observations. Based on the regression model, the multispectral images at the higher spatial resolution of the panchromatic image are optimized by a quadratic programming. In this study, the new method was applied to the IKONOS 1m panchromatic and 4m multispectral data, and the results were compared with them of several current approaches. Experimental results demonstrate that the proposed scheme can achieve significant improvement over other methods.

Key Words : Image Fusion, Pansharpening, Quadratic Programming, Regression Model.

1. Introduction

During the past two decades, technologies acquiring a wide range of remotely-sensed image over the ground surface are maturing to enable routine monitoring for a wide-variety of scientific research and applications related to earth environments. In remote sensing sufficiently high spatial resolution imagery is required for detailed structure on ground surface and it is also necessary for detection of complex features to integrate abundant spectral information. Up to now the satellite imagery with very-high resolution of less than or equal to 1m resolution can be obtained from panchromatic sensors, while multispectral data are available only with mid-high or moderate spatial resolution. Image fusion techniques can effectively integrate the spatial detail of panchromatic data and the spectral characteristics of multispectral images. It is important for human's visual interpretation or computer's autonomous recognition to improve the accuracy in analyzing land-cover types.

The techniques to integrate panchromatic and multispectral data have mainly been developed for the application to generate a RGB image of the higher spatial resolution of the panchromatic image. For this application, the IHS technique (Chavez and Anderson, 1991) and Brovey transform (Civco *et al.*,

Received May 26, 2008; Revised June 10, 2008; Accepted June 22, 2008.

† Corresponding Author: Sang-Hoon Lee (shl@kyungwon.ac.kr)

1995) have been most widely used in practice. The fusion techniques have been designed to obtain the synthetic images similar to the multispectral images that would have been observed from a sensor of the higher resolution. The synthesis process of multispectral images to the higher resolution of the panchromatic image is called "pansharpening" of multispectral images. Zhang and Hong (2005) assorted the algorithms for pansharpening into three categories: 1) projection and substitution methods, such as IHS technique 2) band ratio and arithmetic combination, such as Brovey Transformation, and 3) fusion method which injects spatial features of a panchromatic image into multispectral images. The injection method was earlier developed by using high-pass filtering to extract the spatial features, and later multiresolution analysis such as wavelet and Laplacian pyramids (Yocky, 1995; Nunez *et al.*, 1999; Aiazzi *et al.*, 2002) has been employed for detail injection. The eight algorithms recently developed and provided by seven research teams were compared with a standardized evaluation procedure (Alparone *et al.*, 2007). In their experiments, two algorithms, generalized Laplacian pyramid with context-based decision method (Aiazzi *et al.*, 2002) and additive wavelet luminance proportional method (Otazu, *et al.*, 2005), outperformed all others. They showed that the algorithms based on multiresolution analysis generally performed better than ones based on component substitution.

In this study, a new approach to pansharpening of multispectral imagery is proposed for the synthesis of multispectral images at the higher resolution of the panchromatic image, which agree with the observed spectral values. The proposed scheme reconstructs the multispectral images at the higher resolution using the regression model fitting the panchromatic spectral values to the observed multispectral data. Based on the regression model, pansharpening of multispectral imagery is established as an optimization problem which can be solved a quadratic programming. The new method was applied to the IKONOS 1m panchromatic image of 1200×1200 and 4m multispectral images of 300×300 acquired over the area around Anyang City of Korea. The results were compared to them from the current pansharpening schemes using spatially degraded data.

2. Conventional Techniques for Pansharpening

1) Brovey Transformation

The Brovey transform is based on spectral modeling. Denote P_h be the panchromatic image of h spatial resolution and M_l the image of l spatial resolution ($l < h$). The Brovey transform applies to the digital number of three bands of Red, Green and Blue (RGB). The synthetic image of the i th band, M_h^* is given by

$$\begin{bmatrix} R_h^* \\ G_h^* \\ B_h^* \end{bmatrix} = \frac{3P_h}{R_h' + G_h' + B_h'} \begin{bmatrix} R_h' \\ G_h' \\ B_h' \end{bmatrix} \quad (1)$$

where M_h' is the image resampled M_l at the resolution h.

2) IHS Transformation

The systems widely used to describe a color are RGB system and IHS (Intensity, Hue and Saturation) system, which can convert each other. In the IHS system, the intensity represents the total amount of the light in a color, the hue is the property of the color determined by its wavelength, and the saturation is the purity of the color. Since panchromatic image are acquired across the visible wavelengths, an intensity image of the IHS system is usually similar to a panchromatic image. This property is utilized for pansharpening of the multispectral images with (R,

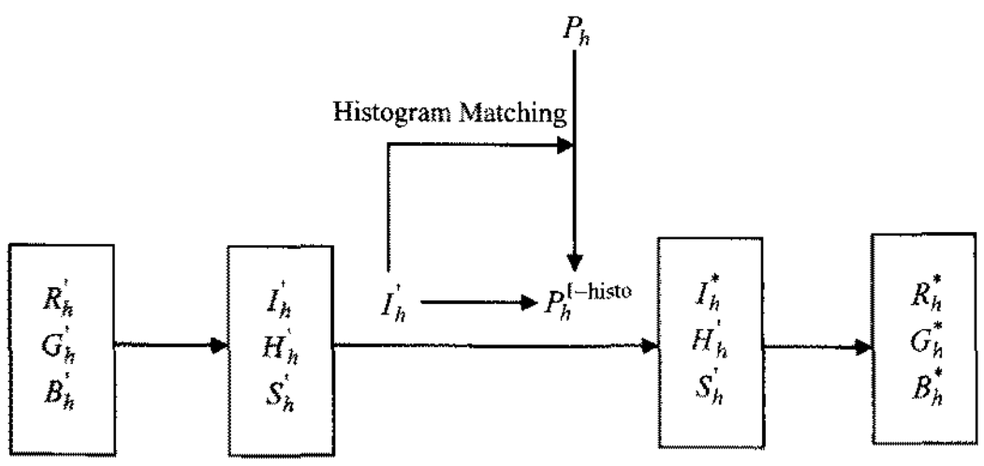

Fig. 1. Outline of IHS pansharpening.

G, B) bands.

For the IHS fusion, the (R, G, B) bands resampled at the scale of the panchromatic image are converted into the IHS components. The smooth intensity component is substituted with the high-resolution panchromatic image. The spectral response of the intensity band may, however, be far different from that of the panchromatic image. For better fusion quality, the panchromatic image is histogram-matched before substitution. The panchromatic image with the hue and saturation images are then reversely transferred from IHS space to RGB space, thereby resulting in a RGB image synthesized at the higher resolution of the panchromatic image. The IHS synthesis process is outlined in Fig. 1.

3) Wavelet Transformation

The wavelet transform, which performs a decomposition of the signal on a base of elementary functions: the wavelets, is utilized as a mathematical tool to detect local features in a signal process. It can be also employed to decompose two-dimensional signals such as digital images into different resolution levels for multiresolution analysis (Mallet, 1989). In the 2-D wavelet multiresolution transform, the original size image (the 1st resolution level) is decomposed with half lower resolution into an "approximation image" (LL^1) and three wavelet coefficients, also called "detailed images" of horizontal (HL^1), vertical (LH^1), and diagonal (HH^1) structures, which contain information of local spatial details. At the successive resolution levels, the approximation images are decomposed into 4 images as shown in Fig. 2. Fig. 3 shows the process of wavelet pansharpening. The three panchromatic images are, first, generated by the histogram matching with (R, G, B) bands respectively, and each panchromatic image is then successively decomposed by the 2-D wavelet transform until the level corresponding to the lower resolution of the multispectral images. After the approximation images at the last level are replaced by the original RGB

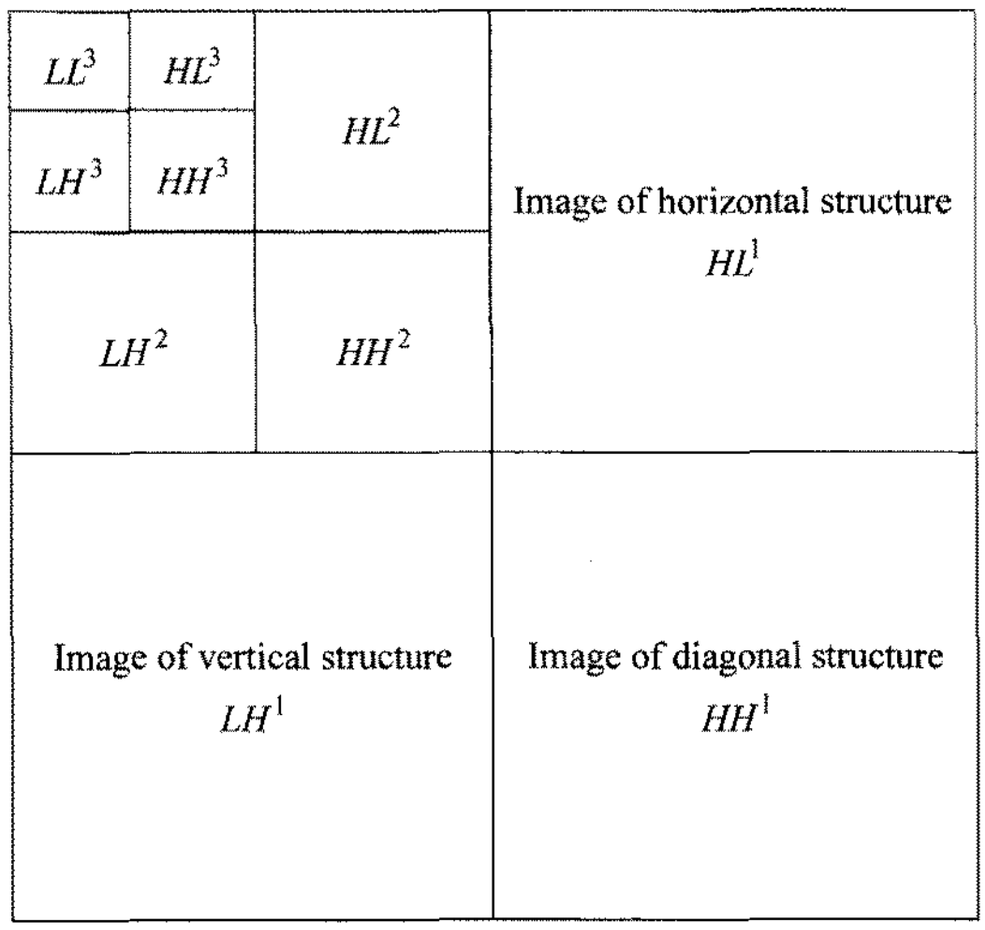

Fig. 2. 2-D Wavelet Multiresolution Transformation.

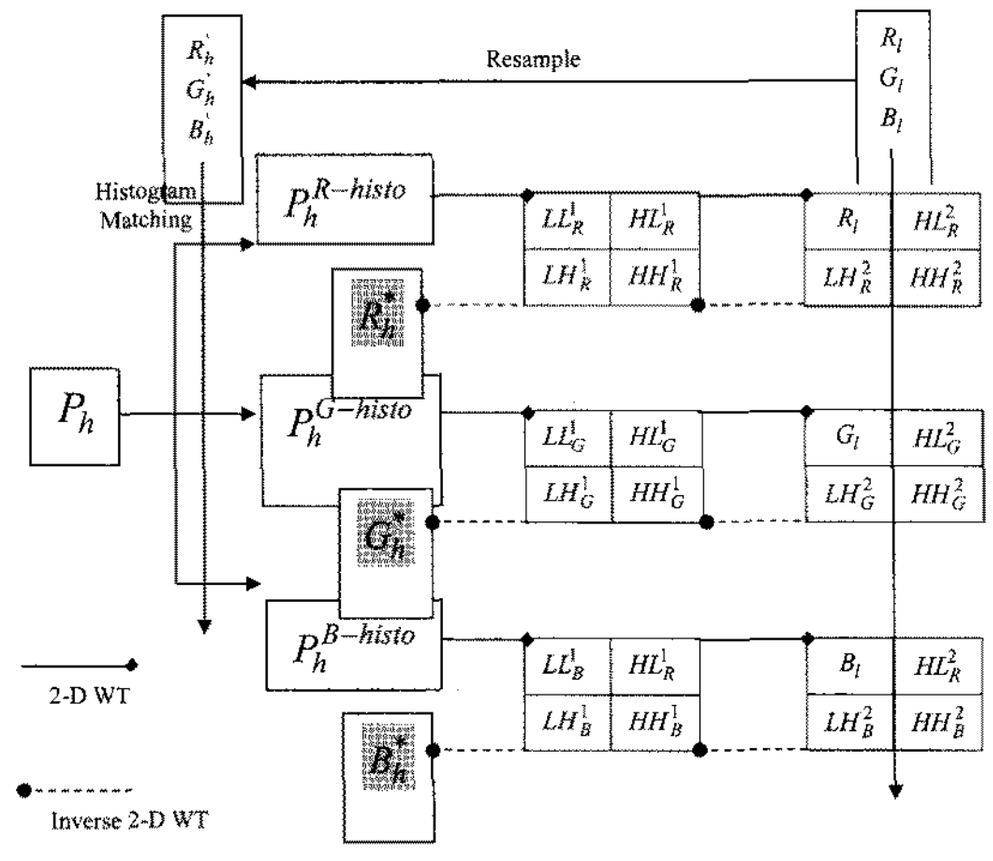

Fig. 3. Wavelet pansharpening.

images, a reverse wavelet transform is applied to each of the sets containing the local spatial details and one of (R, G, B) bands.

3. Quadratic Programming Approach to Pansharpening

In terms of the number of photons, the intensity response of a pixel in the lower resolution is assumed to be equal to the average response of the pixels belonging to the corresponding area in the higher resolution at a same wavelength. Under the assumption, an optimization problem for pansharpening to multispectral imagery is established as the following form: for the i th pixel in one band of the multispectral image of the lower resolution,

$$\underset{z_{i(j)}}{\text{Min}} \sum_{j=1}^{K} (z_{i(j)} - \mu_{i(j)})^2$$

subject to (2)

$$\frac{1}{K}\sum_{j=1}^{K} z_{i(j)} = z_i^{Low}$$

$$lb \le z_{i(j)} \le ub$$

where K is the number of pixels of the panchromatic image corresponding to a pixel of the multispectral image, z_i^{Low} is the observed intensity of the i th pixel in one band of the multispectral images of the lower resolution, $z_{i(j)}$ and $\mu_{i(j)}$ are the estimated and true intensity of the $i(j)$th pixel in a multispectral image of the higher resolution respectively. The th pixel means the jth pixel of the higher resolution belonging to the ith pixel in the lower resolution (see Fig. 4). The lower and upper bounds are given as the constraints by and respectively. The optimization problem of (2) can be rewritten as a quadratic programming (Geil *et al.*, 1991):

1(1)	1(2)	2(1)	2(2)
1(3)	1(4)	2(3)	2(4)
3(1)	3(2)	4(1)	4(2)
3(3)	3(4)	4(3)	4(4)

Fig. 4. Example of pixel indices for lower resolution of 2×2 and higher resolution of 4×4.

$$\underset{z}{\text{Min}} \frac{1}{2}\mathbf{z}^T\mathbf{z} + \mathbf{u}$$

subject to (3)

$$\mathbf{1}^T z = K z_i^{Low}$$

$$\mathbf{b}_l \le \mathbf{z} \le \mathbf{b}_u$$

where $\mathbf{z} = \{z_{i(j)}, j = 1,2,\cdots,K\}$, $\mathbf{u} = \{\mu_{i(j)}, j = 1,2,\cdots,K\}$, $\mathbf{1} = \{1,1,\cdots,1\}$, $\mathbf{b}_l = \{lb,lb,\cdots,lb\}$ and $\mathbf{b}_u = \{ub,ub,\cdots,ub\}$ are all the vectors of K elements. The pansharpened multispectral images are generated by solving the simple quadratic programming of (3) for all the pixels of the multispectral images.

The true intensity is not known, however. The intensity can be estimated based on the observation for the optimization of (2). The main spectral characteristic of panchromatic modality is to cover a broad range of wavelength spectrum including the visible and near-infrared (NIR) wavelength. It is true that the panchromatic response is strongly correlated to the spectral responses of the multispectral bands whose wavelengths range in the panchromatic wavelength spectrum. Fig. 5 shows the scatter plots of the panchromatic band and the (R, G, B) bands of IKONOS data acquired on Anyang area (P_l' vs. M_l where P_l' is the panchromatic image degraded at the scale of the multispectral images and M_l is one of the original multispectral images). These plots show that there exists high correlation between the intensity values of the panchromatic and the multispectral

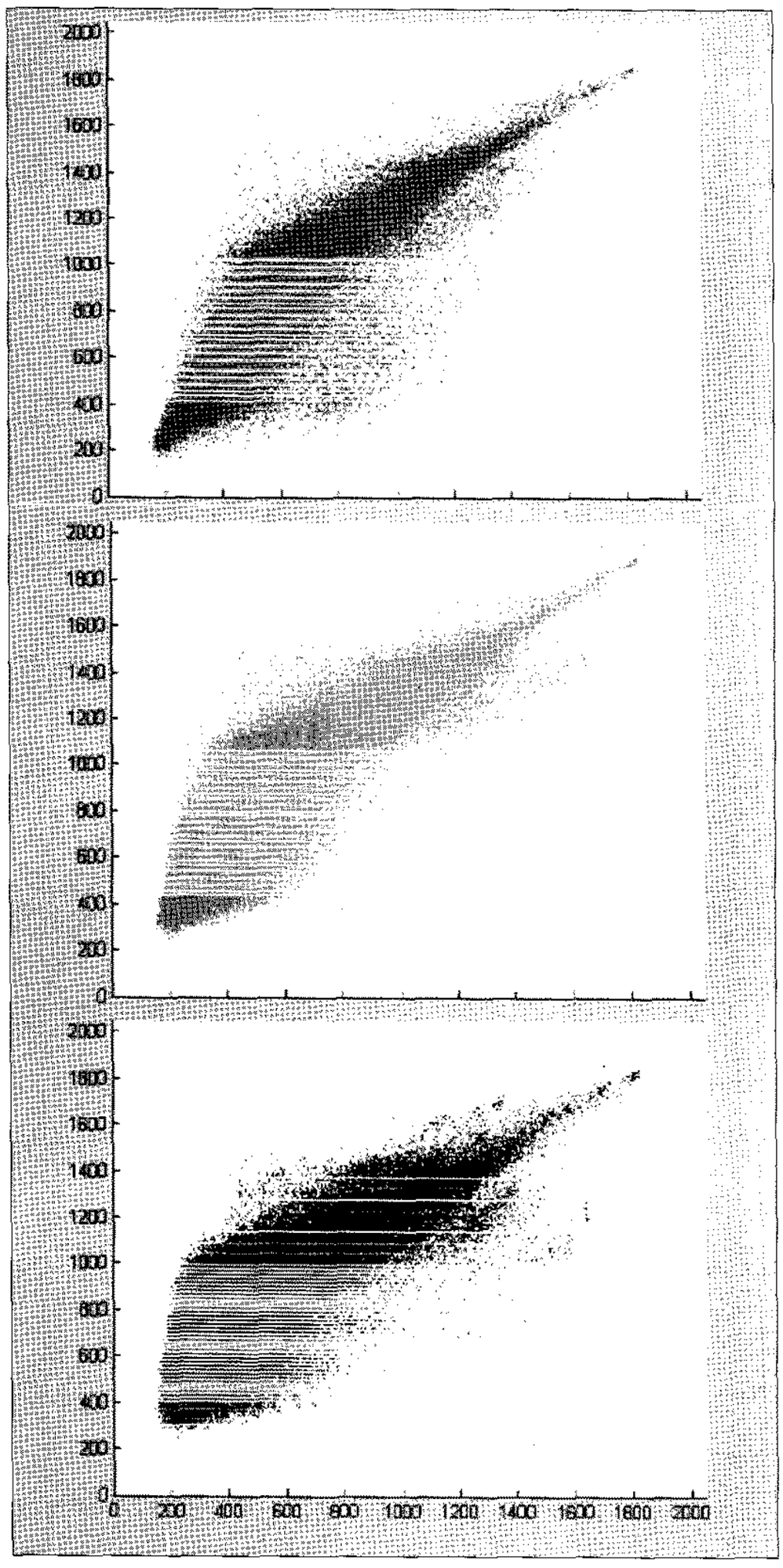

Fig. 5. Scatter plots of panchromatic band and (R, G, B) bands of IKONOS data acquired on Anyang area (from top: R, G, B).

images. From this fact, the true intensity of multispectral images can be considered as a function of panchromatic image. This study employed a polynomial regression model:

$$\begin{Bmatrix} R_l^{True} \\ G_l^{True} \\ B_l^{True} \end{Bmatrix} = \begin{Bmatrix} \beta_0^R + \sum_{k=1}^{m_R} \beta_k^R (P_l')^k \\ \beta_0^G + \sum_{k=1}^{m_G} \beta_k^G (P_l')^k \\ \beta_0^B + \sum_{k=1}^{m_B} \beta_k^B (P_l')^k \end{Bmatrix} \quad (4)$$

where m is the order of polynomial function.

4. Experiments

The proposed method was assessed on IKONOS 1m panchromatic image of 1200×1200 and 4m multispectral images of 300×300 acquired over the area around Anyang City of Korea. The IKONO data of unsigned 11bit range from 0 to 2047.

A performance comparison was carried out among six methods including the proposed QP-FIT scheme:

1) Brovey transformation (BT)
2) IHS transformation (IHS)
3) Wavelet transform (WT)
4) Gram-Schmit spectral sharpening method (GS) as implemented in ENVI (Laben and Brower, 2000)
5) IHS and wavelet integrated approach (IHS-WT) (Zhang and Hong, 2005)
6) The proposed QP-FIT.

A good fused image should satisfy the following conditions (Wald *et al.*, 1997):

1) After that the fused image M_h^* is degraded to its original resolution, it should be as similar as possible to the original image M_l.
2) Any fused image M_h^* should be as identical as possible to the image that would have been observed from the corresponding sensor of the higher resolution.
3) The set of fused multispectral images $\{M_{ih}^*\}$ should be as identical as possible to the set of multispectral images that would have been observed from the corresponding sensor of the higher resolution.

Since the multispectral observation from the corresponding sensor of the higher resolution is not available, it was suggested that the fusion methods are evaluated for the second and third conditions by

applying to the images degraded with the ratio of the lower resolution to the higher resolution (Wald *et al.* 1997). In this experiment, the panchromatic and multispectral images are degraded to 4m and 16m, respectively. Fig. 6 displays the original and degraded RGB images.

Fig. 7 shows the plots of the average values of the multispectral data of the pixels that have the same panchromatic values. The plots in Fig. 7 indicate that the relation between P_l^* and M_l is not linear. In this study, the second order model was employed and estimated by regression analysis. The fitting lines are also displayed in the plots in Fig. 7.

The proposed QP-FIT satisfies the first condition perfectly because it optimized with the constraint $M_h^* = M_l$. For the second condition, Tables 1 and 2 contain the root mean square error (RMSE) and the correlation coefficients (CC) between and M_l for (R, G, B) bands:

$$RMSE(b) = \frac{1}{N_{pixel}} \sum_{\forall i(j)} (z^*_{i(j),b} - z_{i(j),b})^2 \qquad (5)$$

$$CC(b) = \frac{\mathrm{cov}(Z^*_b, Z_b)}{\sigma_{Z^*_b}\sigma_{Z_b}}$$

where $z_{i(j),b}$ and $z^*_{i(j),b}$ are the original and pansharpened values of the $i(j)$ th pixel at the b th band, N_{pixel} is the number of pixels in the higher resolution image, $Z_b = \{z_{i(j),b}\}$ and Z^*_b are the original and pansharpened image of the b the band, and σ_{Z_b} is the standard deviation of Z_b. The CC measures how the contrast of the fused image reflects that of the original image separately, and the RMSE measures the similarity of the fused image to the original image. In the following tables RS indicates the simply resampling at the scale of the higher resolution. As shown in the results of Table 1, BT yielded the pansharpened images much different from the original ones because the panchromatic response are far different from the average spectral values of (R, G, B) bands (the average values of the panchromatic image is 676.6 and the average of RGB images is 976.6). Fig. 8 displays the original panchromatic image and the histogram-matched panchromatic image with the intensity image generated from the IHS transformation of the RGB image. This figure also shows considerable difference in brightness between two images. I-BT is the transformation using the histogram-matched panchromatic image and QP-I-BT is the QP approach using the intensity values of I-BT pansharpened RGB image as the true intensity. QP-FIT, WT, IHS-WT, and QP-I-PT yielded the pansharpened images with better RMSE. Except QP-FIT, the other three methods have much larger RMSE for R band than for G or B bands and larger values, while QP-FIT has much similar RMSEs for all bands. However, the RMSE of B band of QP-FIT is larger than them of the other three methods, because the panchromatic data has somewhat smaller correlation with the B band image (0.8210) than with R (0.9005) and G (0.8770) bands, thereby resulting from less accurate regression model for the true intensity. Table 2 shows the results similar to Table 1 indicating that QP-FIT, WT, IHS-WT, and QP-I-PT performed better.

For the third condition, two different indices of average cumulative quality/distortion are evaluated in Table 3. The first index is *ERGAS* (erreur relative globale adiménsionelle de synthese), which means "dimensionless global relative error of synthesis," defined by

$$ERGAS = \frac{100l}{h} \sqrt{\frac{1}{N_{band}} \sum_{\forall b} \left(\frac{RMSE(b)}{MEAN(b)} \right)^2} \qquad (6)$$

where N_{band} is the number of bands and $MEAN(b) = \sum_{\forall i(j)} z_{i(j),b} / N_{pixel}$ is the mean intensity of the original image of theth band. The capability of *ERGAS* is to measure globally the radiometric distortion in fusion. The second index is based on the

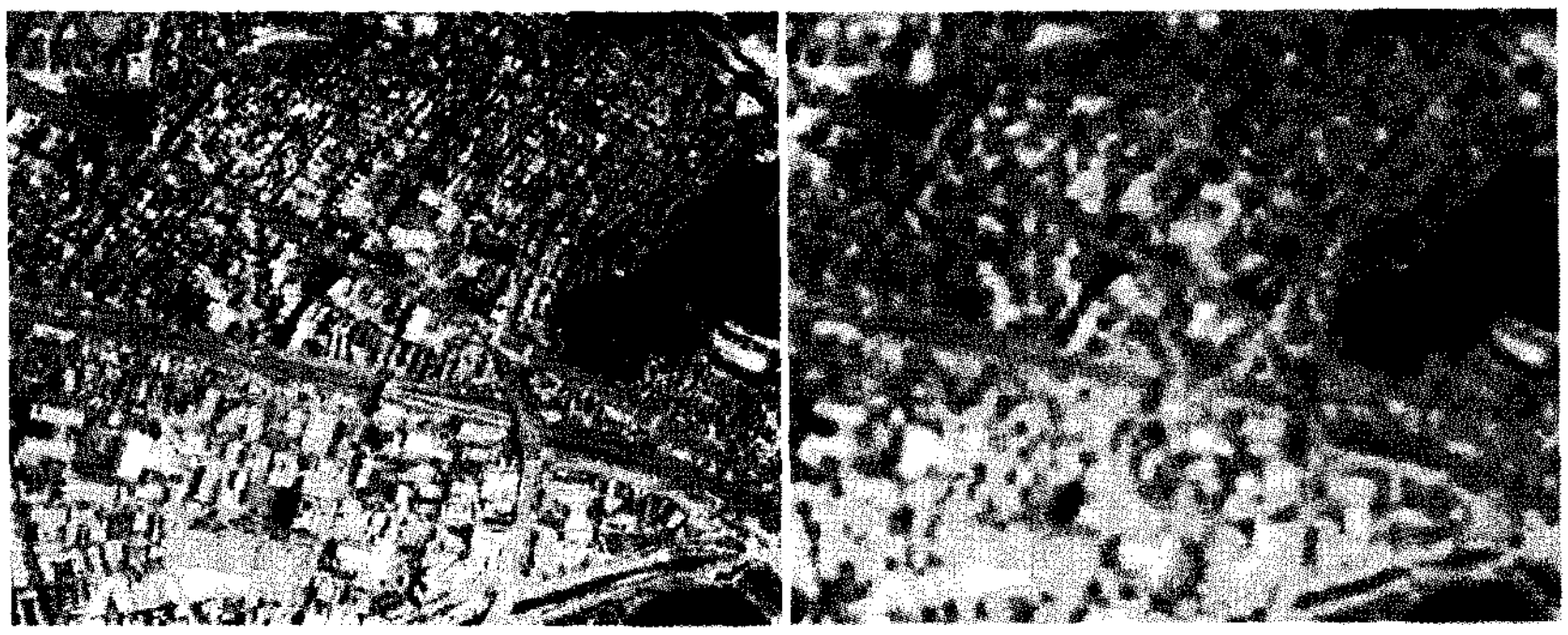

Fig. 6. Original RGB image of 4m resolution and degraded RGB image of 16m resolution.

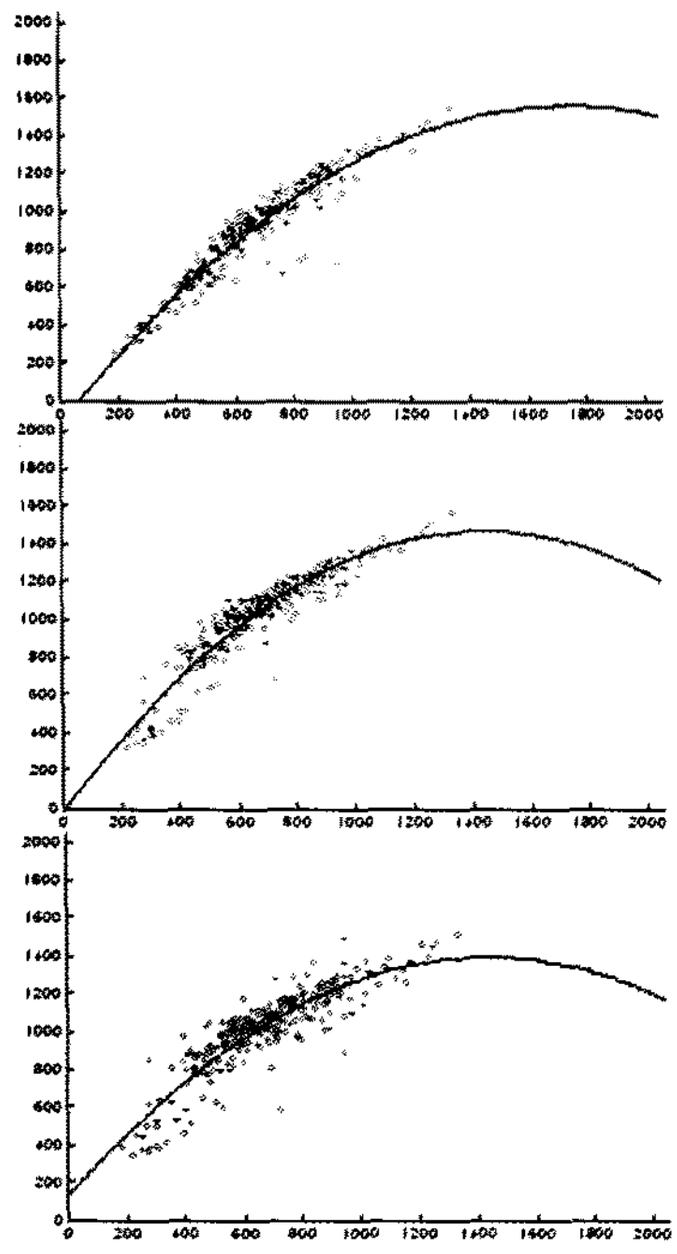

Fig. 7. Plots of average values of (R, G, B) band data of the pixels that have the same panchromatic values (from top: R, G, B).

Table 1. Root Mean Sqaure Errors between 4m original (R, G, B) bands and the pansharpened (R, G, B) bands with 4m panchromatic image and 16m (R, G, B) bands

Method \ Band	R	G	B
RS	242.80	196.58	153.50
BT	312.73	345.32	349.89
IHS	170.55	139.67	142.39
WT	**131.77**	100.96	**94.24**
GS	160.09	135.34	186.60
IHS-WT	137.34	**95.64**	96.75
QP-FIT	**113.26**	99.96	116.83
I-BT	172.57	141.06	141.70
QP-I-BT	138.45	**94.91**	**94.40**

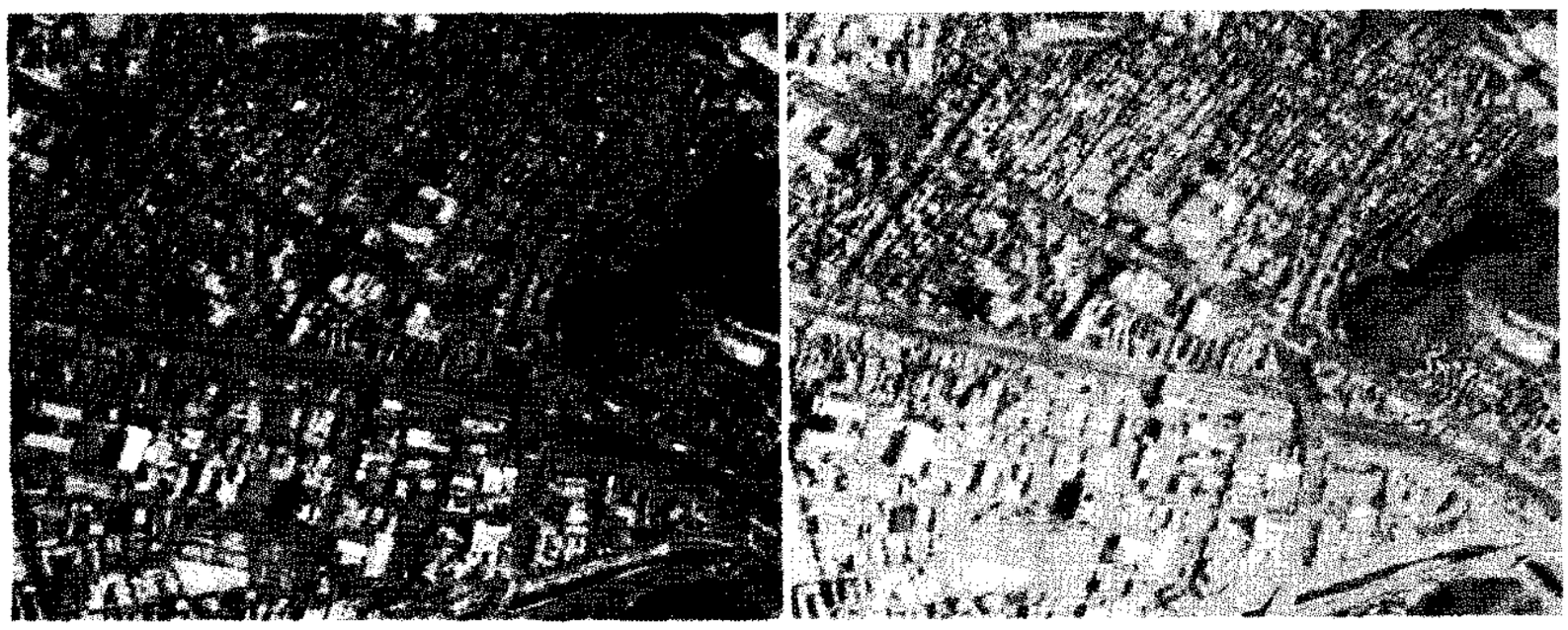

Fig. 8. Original panchromatic image and histogram-matched panchromatic image with intensity image generated from IHS transformation of original RGB image.

Table 2. Correlation Coefficients between 4m original (R, G, B) bands and the pansharpened (R, G, B) bands with 4m panchromatic image and 16m (R, G, B) bands

Band / Method	R	G	B
RS	0.7316	0.7766	0.8214
BT	0.9042	0.8839	0.8455
IHS	0.8994	0.9056	0.8480
WT	**0.9323**	**0.9464**	**0.9371**
GS	0.9158	0.9194	0.9078
IHS-WT	**0.9272**	**0.9520**	**0.9366**
QP-FIT	**0.9478**	**0.9499**	**0.9324**
I-BT	0.8975	0.9032	0.8535
QP-I-BT	**0.9258**	**0.9526**	**0.9393**

Table 3. Average Cumulative Quality/Distortion Indices between 4m original (R, G, B) bands and the pansharpened (R, G, B) bands with 4m panchromatic image and 16m (R, G, B) bands

Index / Method	ERGAS	$\overline{SAM}_{\deg}$
RS	5.2626	1.9965
BT	8.6116	1.9966
IHS	3.9401	1.9631
WT	**2.8834**	**1.7506**
GS	3.6235	1.8115
IHS-WT	2.9297	1.9631
QP-FIT	**2.7295**	**1.5794**
I-BT	3.9600	1.9965
QP-I-BT	2.9225	1.9435

spectral angular mapper (*SAM*) which denotes the absolute value of the spectral angle between two intensity vectors:

$$SAM_{i(j)} = \cos^{-1}\left[\frac{\sum_b (z_{i(j),b}\, z^*_{i(j),b})}{\sqrt{(z^*_{i(j),b})^2}\sqrt{z_{i(j),b})^2}}\right]. \quad (7)$$

A value of $SAM_{i(j)}$ equal to zero denotes absence of spectral distortion, but radiometric distortion is possible. the spectral angular mapper distortion is measured in degrees and averaged over the whole image to yield a global measurement of spectral distortion. The second index is then defined by

$$\overline{SAM}_{\deg} = 90\frac{\sum_{\forall i(j)} SAM_{i(j)}}{N_{pixel}}. \quad (8)$$

For quality assessment for radiometric and spectral distortions, the proposed QP-FIT performed best, WT showed the second performance, and IHS-WT, and QP-I-PT moderately performed.

Fig. 9 displays a 150×150 sub-image of the 1200×1200 original panchromatic observation and the corresponding sub- image of the 300×300 RGB image. For the sub-area in Fig. 9, Fig. 10 displays the resultant RGB images pansharpened by I-BT, GS, IHS, WT, IHS-WT, QP-FIT. It is not easy to distinguish visually quality of the resultant images. The pansharpened images of GS and IHS shows a little smoother color transition compared to the other methods.

5. Conclusions

The new method for pansharpening of multispectral images, QP-FIT was proposed to reconstruct at the higher resolution the multispectral images which agree with the spectral values observed from the sensor of the lower resolution. In the proposed scheme, a regression model represents the relation between panchromatic and multispectral images, and is utilized to estimate the true intensity of multispectral images of the higher resolution based on the multispectral observation. Under the constraint that the intensity response of a pixel in the lower resolution is equal to the average response of the pixels belonging to the corresponding area in the higher resolution at a same wavelength, pansharpening is constructed as an optimization problem which can be solved a quadratic programming. Experiments were carried out on IKONOS data to assess the distortion due to the fusion process for the proposed method by comparing to several current pansharpening

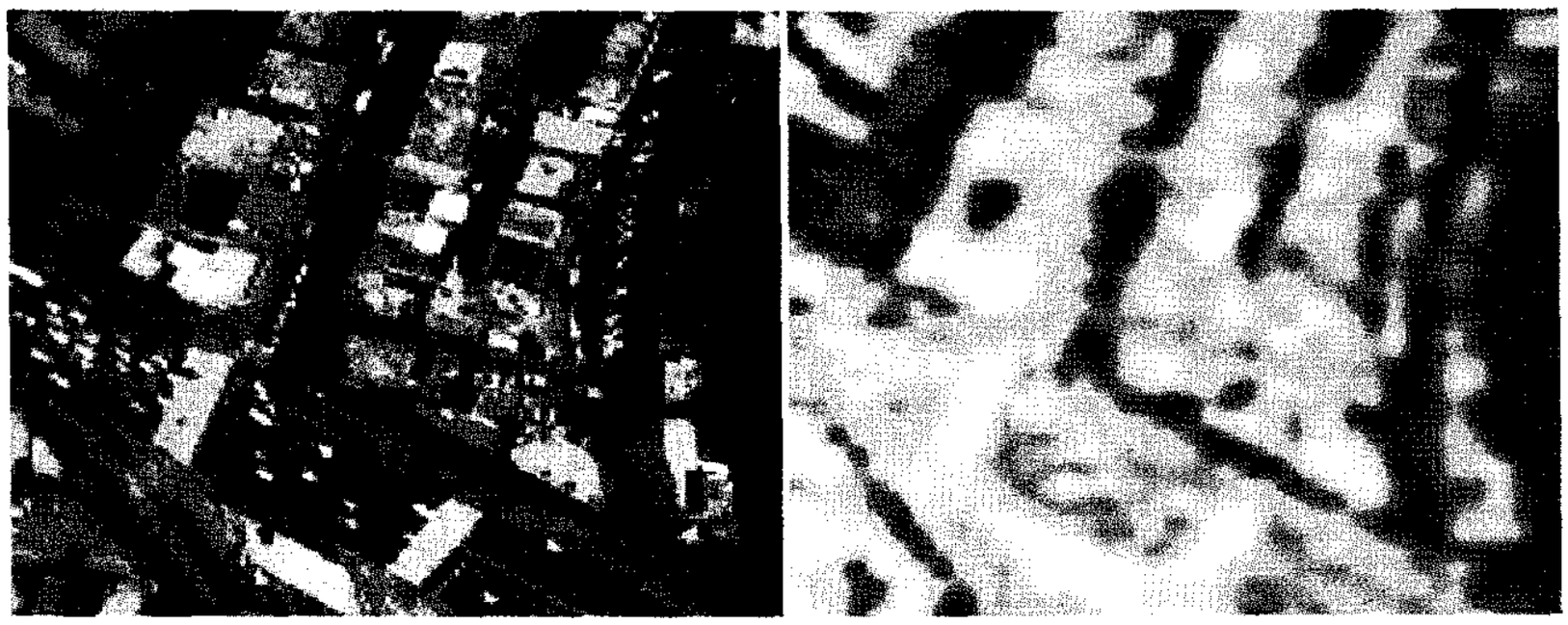

Fig. 9. 150 × 150 sub-image of 1200 × 1200 original panchromatic observation and corresponding sub-image of the 300 × 300 RGB image.

Fig. 10. Resultant RGB images pansharpened by I-BT (top left), GS (top right), IHS (middle left), WT (middle right), IHS-WT (bottom left), QP-FIT (bottom right).

techniques. The results shows that the proposed QP-FIT outperformed over the current techniques considered in the experiments for the statistical analysis with quantitative measures. It was, however, difficult to evaluate quality of the resultant pansharpened image by visual inspection. It is necessary to further extend the experimental study for accurate qualitative assessment of the fusion techniques by visual analysis.

Acknowledgement

This research was supported by a grant(code# 07KLSGC03) from Cutting-edge Urban Development - Korean Land Spatialization Research Project funded by Ministry of Construction & Transportation of Korean government.

References

Aiazzi, B., L. Alparone, S. Baronti, and A. Garzelli, 2002. Context-driven fusion of high spatial and spectral resolution images based on oversampled multiresolution analysis, *IEEE Trans. Geosci. Remote Sens.*, 40: 2300-2312.

Alparone, L., L. Wald, J. Chanussot, C. Thomas, P. Gamba, and L. M. Bruce, 2007. Comparison of pansharpening algoriths: Outcome of the 2006 GRS-S data-fusion contest, *IEEE Trans. Geosci. Remote Sensing*, 45: 3012-3021.

Chavez, P. S., S. C. Sildes, and J. A. Anderson, 1991. Comparison of three different methods to merge multiresolution and multispectral data: Landsat TM and SPOT panchromatic, *Photogramm. Eng. Rem. Sens.*, 57: 295-303.

Civco, D. L., Y. Wang, and J. A. Silander, 1995. Characterizing forest ecosystems in Connecticut by integrating Landsat TM and SPOT panchromatic data, *Proc.1995 Annual ASPRS/ACSM Convention*, Charlotte, NC., 2: 216-224.

Gill, P. E., W. Murray, and M. H. Wright, 1991. *Numerical Linear Algebra and Optimization*, Vol. 1, Addison Wesley.

Laben, C. A. and B. V. Brower, 2000. Process for enhancing the spatial resoltion of multispectral imagery using pan-sharpening, Technical Report US Patent #6,110,875, Eastman Kodak Company.

Mallet, S. G., 1989. A theory for multiresolution signal decomposition: the wavelet representation, *IEEE Trans.Pattern Anal. Mach. Intel.*, 11: 674-693.

Nunez, J., X. Otazu, O. Fors, A. Prades, V. Pala, and R. Arbiol, 1999. Multiresolution-based image fusion with additive wavelet decomposition, *IEEE Trans. Geosci. Remote Sens.*, 37: 1204-1211.

Otazu, X., M. Gonzales Audicana, O. Fors, and J. Nunez, 2005. Introduction of sensor spectral response into image fusion methods: Application to wavelet-based methods, *IEEE Trans. Geosci. Remote Sens.*, 43: 2376-2385.

Wald, L., T. Ranchin, and M. Mangolini, 1997. Fusion of satellite images of different spatial resolutions: Assessing the quality of resulting images, *Photogramm. Eng. Remote Sens.*, 63: 691-699.

Yocky, D. A., 1996. Multiresolution wavelet decomposition image merger of landsat thematic mapper and spot panchromatic data, *Photogramm. Eng. Rem. Sens.*, 69: 1067-1074.

Zhang, Y and G. Hong, 2005. An IHS and wavelet integrated approach to improve pan-sharpening visual quality of natural colur IKONS and QuickBird images, *Information Fusion*, 6: 225-234.